Supporting information

Engineered Sn- and Mg- Doped Hematite Photoanodes for Efficient Photoelectrochemical Water Oxidation

Jiajia Cai[a], Hao Chen[c], Cunxing Liu[a], Shuaiqi Yin[d], Haijin Li[a], Liangcheng Xu[a], Hao Liu[a], Qian Xie[b*]

[a]*School of Energy and Environment, Anhui University of Technology, Ma'sanshan, Anhui, 243002, China*

[b]*School of Metallurgic Engineering, Anhui University of Technology, Ma'anshan, Anhui,243032, China*

[c] *College of Information Science and Engineering, Northeastern University, Shenyang, Liaoning, 110819, China*

[d]*No.2 Steelmaking branch, Zhongtian iron and Steel Group Co., Ltd, Changzhou, Jiangsu, 213011, China*

*Corresponding author: Qian Xie, E-mail: xq.ral@hotmail.com;

The grain size of particles was also calculated using the Scherrer Equation in equation S1.

$$D = K\lambda/(\beta cos\theta) \quad \text{(S1)}$$

Where,

D=cyrstllites size (nm);

K=0.89 (Scherrer constant);

λ=0.15406 nm (wavelength of the X-ray sources);

β=FWHM (Full width at half maximum, radians);

θ=Peak postion (radians);

The grain sizes that calculated from the (104) XRD peak were listed in table S1. The calculated grain sizes were a bit bigger than the ones observed by SEM, which maybe due to the Scherrer Equation is more suitable to calculate the grains that smaller than 100 nm. In spite of this, the grain sizes showed the similar trend with SEM observation, first decreased with Sn doping, and low Mg/Sn doping, then increased with Mg further doping.

Table S1 The grain sizes of particles calculated using Scherrer Equation

	Prinstine α-Fe_2O_3	20Sn α-Fe_2O_3	20Sn/4.5Mg α-Fe_2O_3	20Sn/9.6Mg Fe_2O_3
Grain size(nm)	204	167	132	287

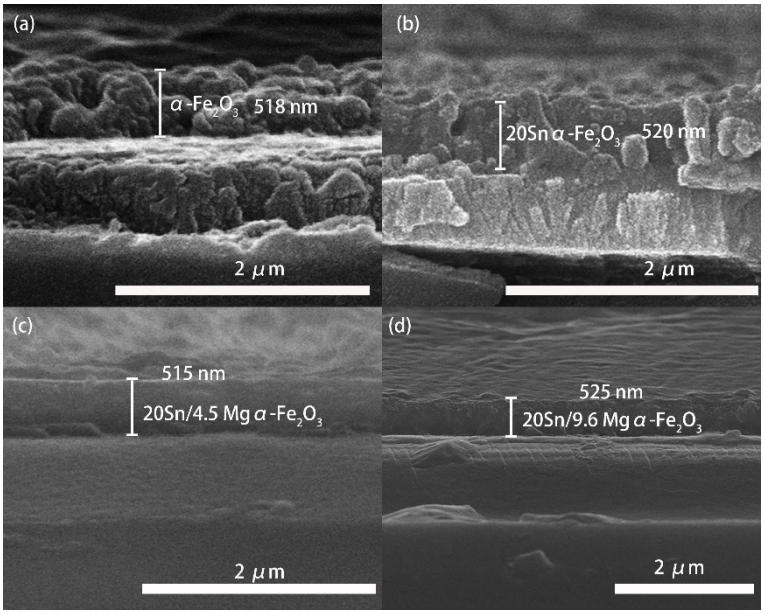

Figure S1 The cross-sectional images of (a) pristine α-Fe_2O_3, (b) 20Sn α-Fe_2O_3, (c) 20Sn/4.5Mg α-Fe_2O_3, (d) 20Sn/9.6Mg α-Fe_2O_3, respectively.

The film thicknesses were 518 nm, 520 nm, 515 nm and 525 nm respectively for pristine α-Fe_2O_3, 20Sn α-Fe_2O_3, 20Sn/4.5Mg α-Fe_2O_3, 20Sn/9.6Mg α-Fe_2O_3, respectively. The nearly similar thickness had little effect on the PEC performance of the films.

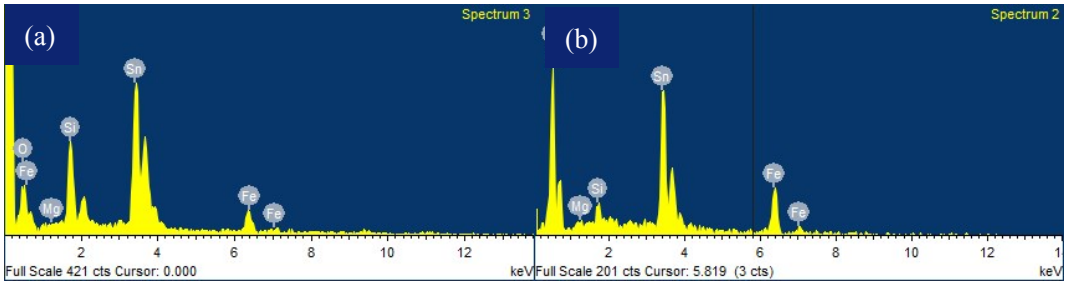

Figure S2 The EDS of (a) 20Sn/4.5Mg co-doping α-Fe_2O_3, (b) 20Sn/9.6Mg co-doping α-Fe_2O_3.

The content of Mg in the co-doping samples were 4.5 at.% and 9.6 at.% respectively.

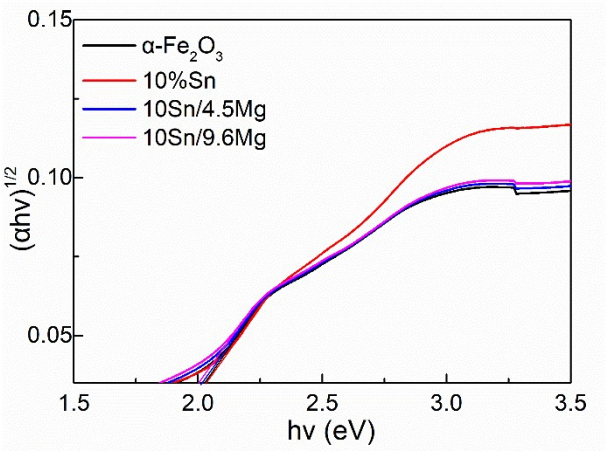

Figure S3 Tauc plots of pristine α-Fe_2O_3, 20Sn doping α-Fe_2O_3, 20Sn/4.5Mg co-doping α-Fe_2O_3, and 20Sn/9.6Mg co-doping α-Fe_2O_3.

The bandgaps of the samples were calculated from the intersection points of the slopes, according to the following relationship:

$$\alpha h\nu \sim (h\nu - E_g)^n \quad \text{(S2)}$$

where α refers to the absorption coefficient, h is the Planck's constant (eV s), ν is the frequency (Hz), E_g refers to the bandgap of the semiconductor, and n is assumed to be 2 for hematite. Therefore, the gotten bandgaps are 2.01 eV, 2.04 eV, 2.02 eV and 2.00 eV for pristine α-Fe_2O_3, 20Sn doping α-Fe_2O_3, 20Sn/4.5Mg co-doping α-Fe_2O_3, and 20Sn/9.6Mg co-doping α-Fe_2O_3, respectively.

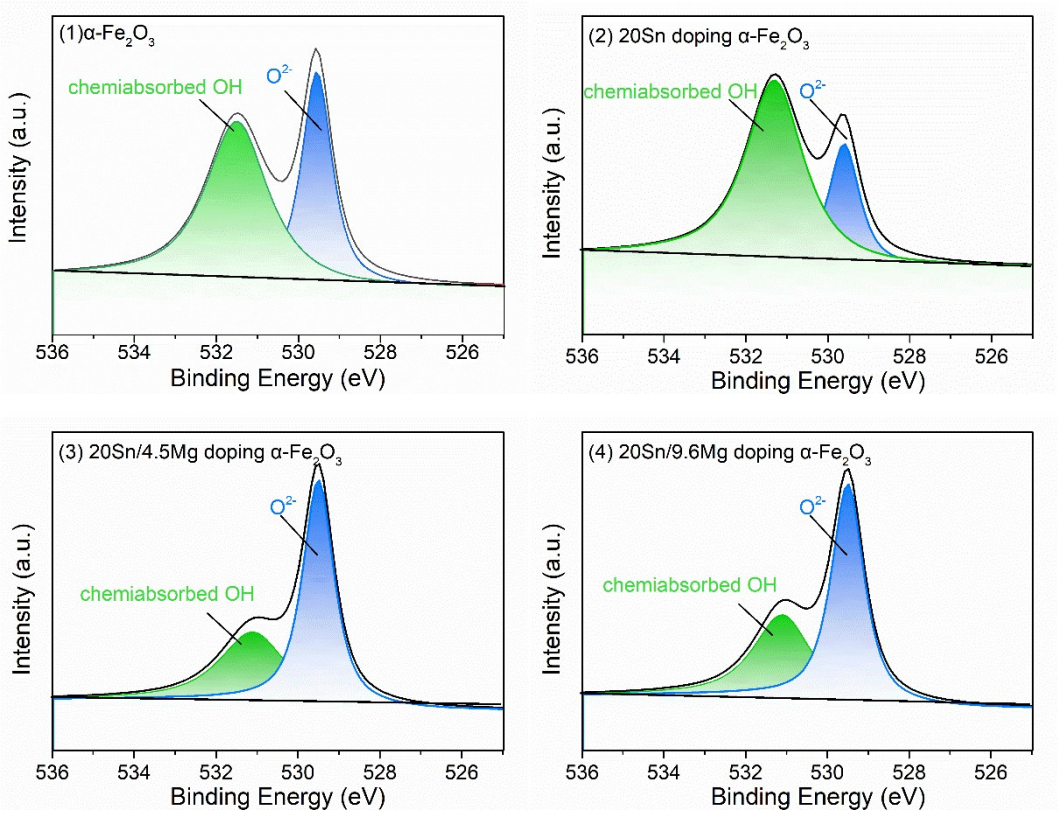

Figure S4 XPS O 1s spectra peaks of chemisorbed OH species, and lattice O^{2-} species (1) pristine α-Fe_2O_3, (2) 20Sn doping α-Fe_2O_3, (3) 20Sn/4.5Mg co-doping α-Fe_2O_3, and (4) 20Sn/9.6Mg co-doping α-Fe_2O_3

Table S2 Summary of XPS peak position and relative abundance of chemisorbed OH species, and lattice O^{2-} species and content of Sn and Mg

Samples	Sn content (at.%)	Mg content (at.%)	lattice O^{2-} (abundance%)	Chemisorbed OH (abundance%)
pristine α-Fe_2O_3	10	n/a	529.6(40%)	531.5(60%)
20Sn doping	20	n/a	529.6(27%)	531.3(73%)
20Sn/4.5Mg co-doping α-Fe_2O_3	20	4.5	529.5(60%)	531.1(40%)
20Sn/9.6Mg co-doping α-Fe_2O_3	20	9.6	529.5(60%)	531.1(40%)

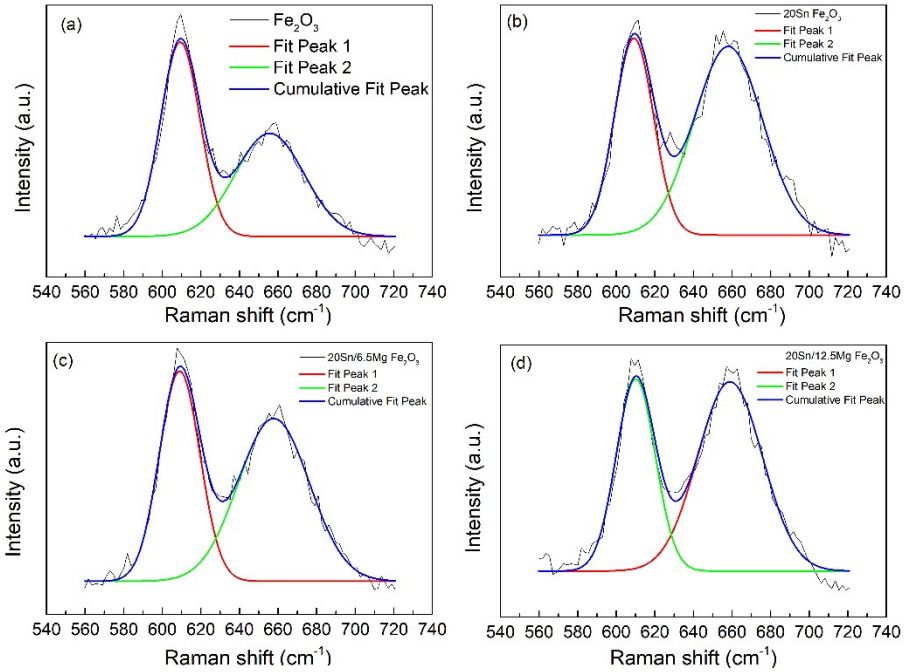

Figure S5 The peak analysis with respect to the $peak_{609}$ and $peak_{656}$ of Raman spectra (1) pristine α-Fe_2O_3, (2) 20Sn doping α-Fe_2O_3, (3) 20Sn/4.5Mg co-doping α-Fe_2O_3, and (4) 20Sn/9.6Mg co-doping α-Fe_2O_3.

Table S3 Raman peak analysis of samples

	$Peak_{609}$ position	$Peak_{609}$ area	$Peak_{656}$ position	$Peak_{656}$ area	Peak area ratio ($Peak_{609}$/ $Peak_{656}$)
pristine α-Fe_2O_3	609	36437	656	33906	0.93
20Sn doping α-Fe_2O_3	609	23928	658	40342	1.69
20Sn/4.5Mg co-doping α-Fe_2O_3	609	33439	658	49679	1.49
20Sn/9.6Mg co-doping α-Fe_2O_3	609	26806	659	43926	1.64

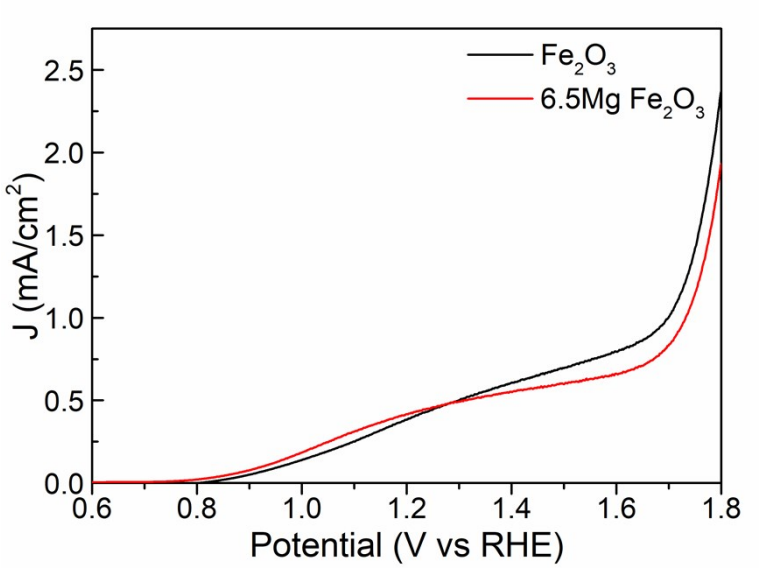

FigureS6 J-V curves pristine and Mg doped α-Fe_2O_3 photoanodes measured in the NaOH

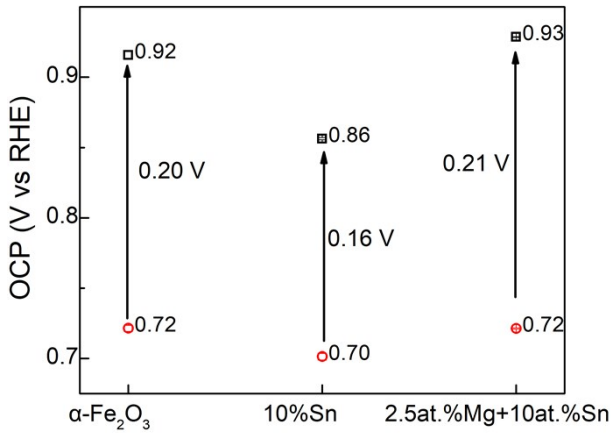

Figure S7 Open-circuit potential measurements in the dark and under illumination for pristine, 20Sn and 20Sn/9.6Mg doping α-Fe_2O_3 in the 1 M NaOH. The black hollow cubic represent the OCP in dark, and the red hollow circles represent the OCP under illumination

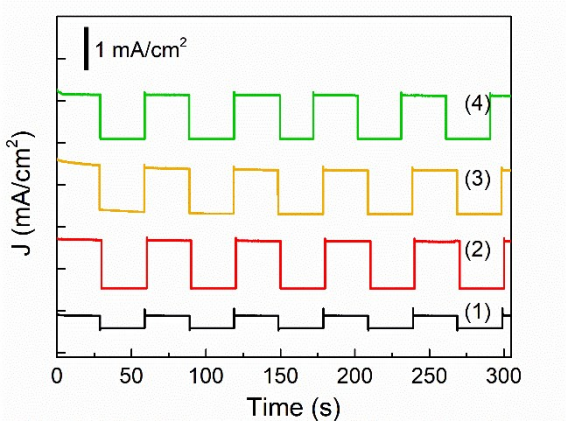

Figure S8 Chronoamperometric measurement of samples at 1.6 V_{RHE} (1) pristine α-Fe_2O_3, (2) 20Sn doping, (3) 20Sn/4.5Mg co-doping α-Fe_2O_3, and (4) 20Sn/9.6Mg co-doping α-Fe_2O_3

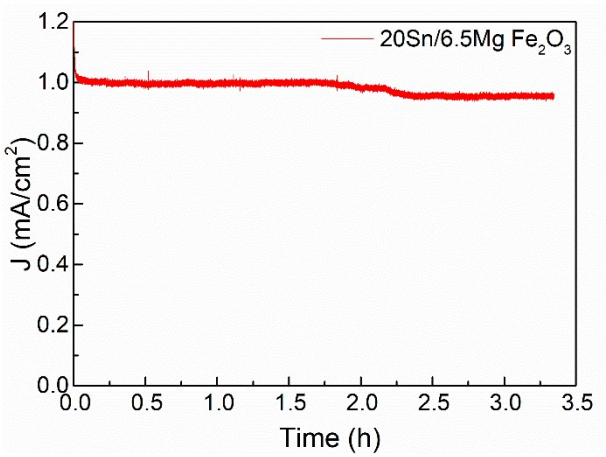

Figure S9 Photocurrent density-time curve of the 20Sn/4.5Mg co-doping α-Fe_2O_3 at 1.23 V vs RHE under illumination

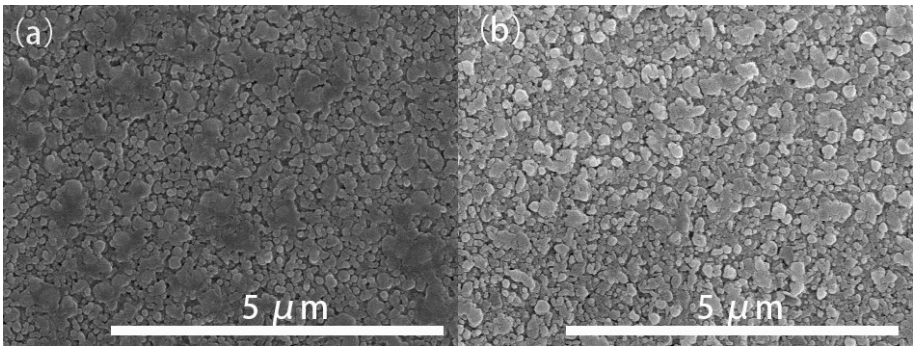

FigureS10 SEM images of (a) pristine and (b) 20Sn/4.5Mg co-doping α-Fe_2O_3 after PEC test

The faradaic efficiency of sample 20Sn/4.5Mg co-doping α-Fe_2O_3 was measured in by testing the volume of O_2 gas during the i-t measurement at 1.33 V vs RHE for 5000 s. The schematic of homemade gas gathering equipment was shown both below and in Figure S9 in the supporting information.

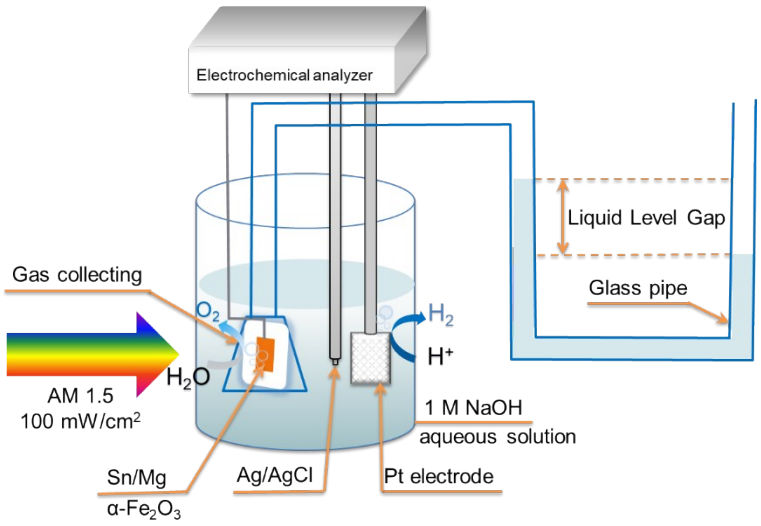

Figure S11 Schematic of a custom-built reactor for gas test

Faradaic efficiency was calculated using the Eq.S3[1].

$$Faradaic\ efficiency = \frac{experimental\ mol\ of\ O_2\ gas}{theoretical\ mol\ of\ O_2\ gas} \times 100 \quad \text{(S3)}$$

The theoretical amount of O_2 gas was calculated from Faraday's law Eq.S4

$$n = \frac{I \times t}{z \times F} \times 100 \quad \text{(S4)}$$

Where, n is the number of mole, I is the current, t is the time, z is the transfer of electrons(z=4 for O_2), and F is the Faraday constant(96485 C/mol), the calculation detail can be seen in the previous reference[1].

During the 5000 s, the practical mole of oxygen was 0.849 μmol, and the theoretical value was 0.928 μmol. By calculation, the faradaic efficiency for O_2 was 92%.

Table S4 Photocurrent density and onset potential different hematite PEC water splitting

Samples	E_{onset}	$J_{1.23VRHE}$	Ref
Co_3O_4 loaded $CaFe_2O_4/Fe_2O_3$	0.69	0.095	[2]
α-Fe_2O_3/NiMn layered double hydroxide	0.65	1.98	[3]
Al_2O_3 coated Fe_2O_3	0.90	0.04	[4]
Sn/P co-doping	0.68	0.90	[5]
Sn doped α-Fe_2O_3	0.7	1.04	[6]
20Sn/4.5Mg co-doping α-Fe_2O_3	0.93	1.10	This work

Table S5 Summary of PEC analysis results (comparison of J_{ph} at 1.23 V vs RHE($J_{1.23\ V}$), onset potential(E_{onset}, estimated with J_{ph}=0 intersect method), potential of maximum power efficiency(E_{Wmax}) and the corresponding efficiency $ABPE_{max}$

Samples	E_{Wmax}	$ABPE_{max}$(%)	E_{onset}	$J_{1.23VRHE}$
pristine α-Fe_2O_3	1.1	0.03	0.89	0.42
20Sn doping	1.1	0.07	0.94	0.78
20Sn/4.5Mg co-doping α-Fe_2O_3	1.1	0.09	0.93	1.1
20Sn/9.6Mg co-doping α-Fe_2O_3	1.1	0.07	0.92	0.92

References

1 S. Sultan, M. Ha, D. Y. Kim, J. N. Tiwari, C. W. Myung, A. Meena, T. J. Shin, K. H. Chae and K. S. Kim, *Nat Commun*, 2019, **10**, 5195.

2 J. Cai, S. Li and G. Qin, *Applied Surface Science*, 2019, **466**, 92–98.

3 X. Yu, J. Liu, W. Yin, T. Wang, L. Quan, Y. Ran, J. Cui, L. Wang and Y. Zhang, *Applied Surface Science*, 2019, **492**, 264–271.

4 W. Jiao, J. Wu, S. Cui, N. Wei, Z. U. Rahman, M. Yu, S. Chen, Y. Zhou and D. Wang, *Dalton Trans.*, 2017, **46**, 10635–10640.

5 S. F. Duan, Y. Y. Geng, X. B. Pan, X. Q. Yao, Y. X. Zhao, X. Li, C. L. Tao and D. D. Qin, *Dalton Trans.*, 2019, **48**, 928–935.

6 J. W. Park, A. Subramanian, M. A. Mahadik, S. Y. Lee, S. H. Choi and J. S. Jang, *Dalton Trans.*, 2018, **47**, 4076–4086.